Bio-Design and Manufacturing (2022) 5:318–332
https://doi.org/10.1007/s42242-021-00172-1

RESEARCH ARTICLE

Injectable bioactive polymethyl methacrylate–hydrogel hybrid bone cement loaded with BMP-2 to improve osteogenesis for percutaneous vertebroplasty and kyphoplasty

Xin Sun[1] · Xin Zhang[2] · Xin Jiao[1] · Jie Ma[1] · Xingzhen Liu[1] · Han Yang[2] · Kangping Shen[1] · Yaokai Gan[1] · Jinwu Wang[1] · Haiyan Li[2,3] · Wenjie Jin[1]

Received: 18 April 2021 / Accepted: 24 October 2021 / Published online: 25 January 2022

Abstract

Polymethyl methacrylate (PMMA) bone cement is used in augmenting and stabilizing fractured vertebral bodies through percutaneous vertebroplasty (PVP) and percutaneous kyphoplasty (PKP). However, applications of PMMA bone cement are limited by the high elasticity modulus of PMMA, its low biodegradability, and its limited ability to regenerate bone. To improve PMMA bioactivity and biodegradability and to modify its elasticity modulus, we mixed PMMA bone cement with oxidized hyaluronic acid and carboxymethyl chitosan in situ cross-linking hydrogel loaded with bone morphogenetic protein-2 (BMP-2) to achieve novel hybrid cement. These fabricated PMMA–hydrogel hybrid cements exhibited lower setting temperatures, a lower elasticity modulus, and better biodegradability and biocompatibility than that of pure PMMA cement, while retaining acceptable setting times, mechanical strength, and injectability. In addition, we detected release of BMP-2 from the PMMA–hydrogel hybrid cements, significantly enhancing in vitro osteogenesis of bone marrow mesenchymal stem cells by up-regulating the gene expression of *Runx2*, *Col1*, and *OPN*. Use of PMMA–hydrogel hybrid cements loaded with BMP-2 on rabbit femoral condyle bone-defect models revealed their biodegradability and enhanced bone formation. Our study demonstrated the favorable mechanical properties, biocompatibility, and biodegradability of fabricated PMMA–hydrogel hybrid cements loaded with BMP-2, as well as their ability to improve osteogenesis, making them a promising material for use in PKP and PVP.

Xin Sun and Xin Zhang have contributed equally to this work and are joint first authors.

Jinwu Wang, Haiyan Li, and Wenjie Jin have contributed equally to this work and are joint corresponding authors.

✉ Jinwu Wang
wangjw-team@shsmu.edu.cn

✉ Haiyan Li
haiyan.li@sjtu.edu.cn

✉ Wenjie Jin
surgeonjin@126.com

Xin Sun
sunxinspine@sina.com

Xin Zhang
zhangxinsjtu@sjtu.edu.cn

Xin Jiao
jiaoxin2020@126.com

Jie Ma
doctorjack@163.com

Xingzhen Liu
spine2009@sina.com

Han Yang
yanghan0609@sjtu.edu.cn

Kangping Shen
shkp2016@163.com

Yaokai Gan
ganyk2004@126.com

1 Shanghai Key Laboratory of Orthopaedic Implants, Department of Orthopaedic Surgery, Shanghai Ninth People's Hospital, Shanghai Jiao Tong University School of Medicine, Shanghai 200001, China

2 School of Biomedical Engineering, Shanghai Jiao Tong University, Shanghai 200030, China

3 Chemical and Environmental Engineering, School of Engineering, RMIT University, 124 La Trobe St., Melbourne, VIC 3000, Australia

Graphic abstract

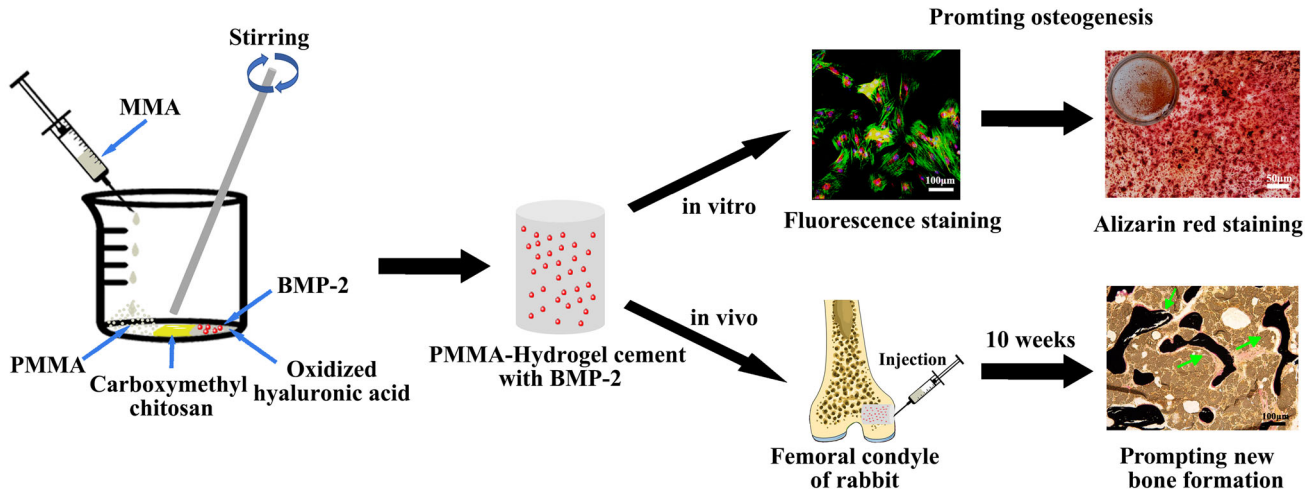

Keywords Polymethyl methacrylate bone cement · Hydrogel · Bone morphogenetic protein-2 · Osteogenesis · Percutaneous vertebroplasty

Introduction

Osteoporotic vertebral compression fractures (OVCFs) are a major health challenge for the elderly after spinal trauma. OVCFs can lead to sustained low back pain and further long-standing convalescence, thereby hindering daily activities and reducing quality of life [1–3]. About 1.4 million new cases of OVCF are reported each year in Europe, along with 750,000 new cases annually in the USA [4, 5]. To date, percutaneous kyphoplasty (PKP) and percutaneous vertebroplasty (PVP) involving the injection of polymethyl methacrylate (PMMA) bone cement are the standard minimally invasive treatments for OVCFs, helping to stabilize fractured vertebral bodies and relieve back pain [1–3]. Owing to the various advantages of PMMA cement, such as easy injection, high mechanical support, and low cost, it is the most commonly used and most extensively investigated clinical treatment [6, 7]. However, PMMA cement has several disadvantages, including excessive elastic modulus, a high setting temperature, and low degradability [6, 7]. In addition, PMMA cement does not promote osteogenesis, osteoconduction, or osseointegration, possibly resulting in delayed union or non-union of fractures [6, 8, 9]. Further, loosening of PMMA cement may result in its protrusion from fractured vertebral bodies, causing neurological dysfunction and vascular injury after a second trauma, thereby prompting the need for additional repair surgery [6, 8, 10]. Therefore, it is important to improve the material characteristics and bioactivity of PMMA cement to optimize the effectiveness of its extensive clinical applications in PVP and PKP for treatment of OVCFs.

To overcome the limitations of PMMA cement, particularly in promoting osteogenesis, several researchers have investigated the effect of adding inorganic materials, such as bioactive glass, silicate bioceramics, and hydroxyapatite (HA) [6, 11, 12]. The resulting hybrid bone cement can reduce the elasticity modulus and setting temperature, modify biodegradability, and accelerate new bone formation around the hybrid cement for its use in osteogenesis [6, 11, 12]. Therefore, addition of bioactive materials to PMMA cement has attracted attention as a potential focus for research investigation. However, only small amounts of inorganic material can be used in hybrid bone cement, because excessive inorganic content can have potentially adverse effects on physicochemical properties of the cement, such as injectability, mechanical strength, and setting time [11–13]. In addition, inorganic materials have weaker effects on osteogenesis than bioactive factors, such as bone morphogenetic proteins (BMPs). However, the setting temperature of pure PMMA cement is greater than 60 °C, a temperature that will inactivate bioactive factors, and there is not a suitable alternative liquid environment for incorporating these factors into PMMA [6, 14]. Thus, to date, there have been no published analyses of PMMA cements containing bioactive factors.

Several recent studies have reported that addition of an appropriate percent of hydrogel (e.g., gelatin, carboxymethylcellulose, or chitosan) to PMMA results in successful setting of the cement [15–17]. In particular, addition of a hydrogel to PMMA cement can provide a suitable liquid environment and significantly reduce the setting temperature, which is important for effective loading of bioactive

factors [15–17]. Moreover, the gradual degradation of hydrogels in hybrid bone cement supports the continuous release of the loaded bioactive factors [18]. Oxidized hyaluronic acid and carboxymethyl chitosan can undergo in situ cross-linking without changes in temperature, pH, and chemical addition, thereby avoiding changes in physical and chemical conditions that may disrupt hydrogel cross-linking and the setting of PMMA cement in vivo [19, 20]. Accordingly, in this study, oxidized hyaluronic acid and carboxymethyl chitosan composite hydrogel were mixed with PMMA cement.

Bone morphogenetic protein-2 (BMP-2) is one of the most common osteogenic agents proven to promote osteogenesis [21, 22]; it also upregulates the expression of alkaline phosphatase (ALP), osteocalcin, and osteopontin (OPN) through the Smad1/5/8 signaling pathway, accelerating the osteogenic differentiation of bone marrow mesenchymal stem cells (BMSCs) and osteoblasts [21, 22]. Thus, in this study, we have proposed the use of oxidized hyaluronic acid and carboxymethyl chitosan cross-linked in situ to form a hydrogel into which BMP-2 can be incorporated. We subsequently synthesized a novel PMMA–hydrogel hybrid cement with bioactive factors. After evaluating its physicochemical characteristics, biocompatibility, BMP-2 release, and osteogenic potential in vitro, and the in vivo formation of new bone tissue, we confirmed the potential of this PMMA–hydrogel hybrid cement loaded with BMP-2 for use in PVP and PKP.

Materials and methods

Preparation of PMMA with oxidized hyaluronic acid and carboxymethyl chitosan hydrogel hybrid cements

Liquid methyl methacrylate (MMA) and powdered PMMA were purchased from TecresSpA (Mendec Spine®, TecresSpA, Verona, Italy). Carboxymethyl chitosan was purchased from Macklin (C804727, Macklin, Shanghai, China). Oxidized hyaluronic acid was prepared as previously described [20]. Briefly, 5 g of hyaluronic acid was added to 500 mL of ultrapure water and stirred at room temperature (25 °C) until it was completely dissolved. Subsequently, 1 g of sodium periodate was dissolved in 5 mL of ultrapure water and the solution added dropwise into the hyaluronic acid solution in the dark. The mixed solution was stirred in the dark for 24 h before adding 2 mL of ethylene glycol to stop the reaction. The obtained reaction solution was placed in a dialysis bag (MWCO 7000) in ultrapure water for 3 days, with the water changed three times per day. Finally, the solution was frozen in an ultra-low temperature freezer (-80 °C) and vacuum freeze-dried to obtain solid oxidized hyaluronic acid.

Pure PMMA cement with a PMMA:MMA ratio of 2 g:1 mL was prepared according to [6]. PMMA and 5%–25% hydrogel (volume of 5% w/v oxidized hyaluronic acid or 5% w/v carboxymethyl chitosan/MMA) hybrid cement was also prepared (Table S1 in Supplementary Information) (Note on nomenclature: the PMMA–5% Hydrogel group denotes 50 μL oxidized hyaluronic acid and 50 μL carboxymethyl chitosan with 2 g PMMA and 1 mL MMA). The PMMA–hydrogel hybrid cement was fabricated by the following procedure (Fig. 1): First, oxidized hyaluronic acid, carboxymethyl chitosan, and PMMA were each added to a sterile bottle at 25 °C. If needed, according to the composition of the different groups, BMP-2 was added to the oxidized hyaluronic acid. MMA was then quickly added to the PMMA. Finally, the mixture was blended by constant stirring for 1 min to create a homogeneous paste, which was then cast in Teflon molds to construct the different samples (cylindrical, $\Phi = 6$ mm, $H = 2$ or 12 mm).

Material characterization of PMMA–hydrogel hybrid cements

To characterize the different fabricated PMMA–hydrogel hybrid bone cements, the setting temperature was first evaluated using a type K thermocouple (Testo, Lenzkirch, Germany) at 25 °C. Next, the compressive strength of the different specimens ($\Phi = 6$ mm, $H = 12$ mm) was evaluated using a universal testing machine (Shimadzu Corporation, Japan) with a crosshead speed of 0.5 mm/min and maximum stroke displacement of 4 mm [6]. The injectability of each cement type was then assessed by manually extruding an amount of paste through a syringe and calculating injectability with the following equation: injectability (%) = paste weight extruded from the syringe/total weight before extrusion × 100% [6]. Next, the initial and final setting times were evaluated using a Vicat apparatus according to ISO-9597-2008E. Finally, after thoroughly drying the PMMA–hydrogel hybrid cement specimens at 60 °C, the original weight (m_0) was recorded, and the specimens were then soaked in simulated body fluid (SBF; Leagene Biotechnology, Beijing, China) with a specimen surface area/soaking solution ratio of 0.1 cm^2/mL at a shaking speed of 120 r/min under saturated humidity at 37 °C. After soaking for 3, 7, 14, 21, and 28 days, specimens were removed from the solution, rinsed with ultrapure water, and then dried. The final weight (m_x) was recorded. Degradation was calculated using the following equation: degradation (%) = $[(m_0 - m_x)/m_0] \times 100\%$. The other three specimens that were soaked for 14 and 28 days were evaluated using scanning electron microscopy (SEM, S-4800, Hitachi, Japan) to observe degradation. Three samples apiece were evaluated for each of the above tests.

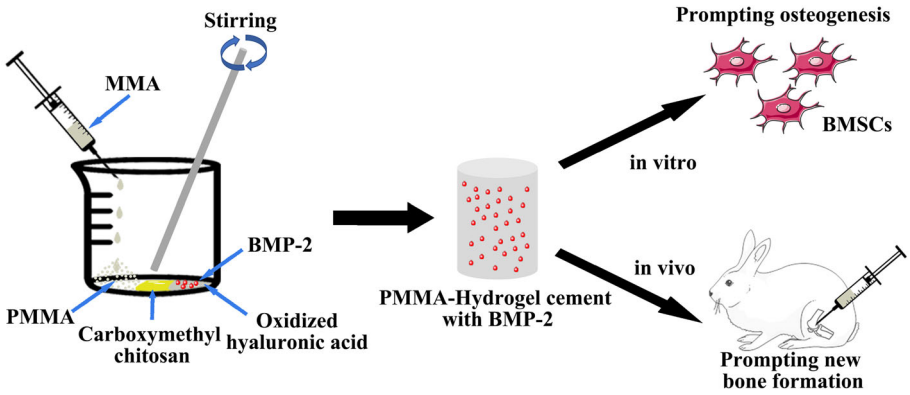

Fig. 1 Study design. Oxidized hyaluronic acid, carboxymethyl chitosan, and PMMA were independently added to a sterile bottle; in some experimental groups, BMP-2 was added to the oxidized hyaluronic acid. MMA was then quickly added to the PMMA. Finally, the mixture was blended by stirring for 1 min to build a homogeneous paste and samples were cast to perform in vitro and vivo analyses

Primary BMSCs isolation and culture

All animal culture procedures and the use of animals in our experiments complied with the guidelines of the National Institutes of Health Guide for Care and Use of Laboratory Animals (GB14925-2010), and were approved by Shanghai Ninth People's Hospital, Shanghai Jiao Tong University School of Medicine Animal Care and Use Committee. Healthy, three-week-old male Sprague Dawley (SD) rats ($n = 5$) were purchased from the Animal Laboratory of Shanghai Jie-Si-Jie Co. (Shanghai, China). All rats were sacrificed and immersed in 75% alcohol for 5 min. Next, the soft tissue was dissected from the lower limbs on a clean worktable under sterile conditions. The entire marrow was flushed out thoroughly using phosphate buffered saline (PBS), filtered with a 70-μm nylon mesh filter, and centrifuged. BMSCs were cultured in α-MEM medium (Hyclone, Logan, UT, USA) with 10% fetal bovine serum (Gibco, Paisley, UK), 1% penicillin–streptomycin (Hyclone), and 0.4% gentamicin (Sangon Biotech, Shanghai, China), and the solution was replaced every 3–4 days. Cell culture passage numbers of 3–5 were routinely used for this study.

Cell culture and cytocompatibility evaluation

Extracts of PMMA–hydrogel hybrid cement variants and pure PMMA were prepared according to a previous report [23]. Sterile cement samples were immersed in serum-free α-MEM medium (0.2 g/mL) at 37 °C for 24 h. Cell Counting Kit 8 (CCK-8; Beyotime, Shanghai, China) and Live-Dead staining (KeyGEN, Nanjing, China) were used to determine cell proliferation and cytocompatibility on days 1, 3, 5, and 7, following the respective manufacturers' instructions. For the CCK-8 test, BMSCs were seeded into 96-well plates at a density of 10^4 cells per well for 24 h. The medium was then replaced with the above extracts; at each time point, the extracts were removed and replaced by a solution of 100 μL of fresh medium and 10 μL of CCK-8 in each well, followed by incubation for 2 h. The final supernatant was collected and its absorbance evaluated using an enzyme-linked immunoadsorbent assay (ELISA) microplate reader (Synergy 2, Bio-TEK, Vermont, USA) at 450 nm. For Live-Dead staining, BMSCs were seeded into 24-well plates at a density of 3×10^4 cells per well for 24 h. Next, the medium was replaced with the above extracts, and the cells were visualized with Live-Dead staining at 37 °C for 30 min at each time point. Finally, the cells were rinsed two times with PBS and observed by fluorescence microscopy. Cell viability was calculated from images using the following equation: cell viability (%) = number of live cells/number of total cells × 100%. Each of the above experiments was conducted in triplicate.

Hemolysis test

Hemolysis experiments were performed to measure hemocompatibility of the specimens in vitro [24]. Rabbit blood samples were collected in ethylenediaminetetraacetic acid tubes. A 1 mL sample was then added to 2 mL PBS, and centrifuged at 4000 r/min for 10 min to isolate the red blood cells from the serum. After washing five times, the volume of blood was diluted to 1/10 with SBF. Next, 0.2 mL of the diluted suspension was blended with (a) 0.8 mL SBF solution as the negative control, (b) 0.8 mL ultrapure water as the positive control, and (c) cement specimens (pure PMMA cement, PMMA–15% hydrogel, and PMMA–20% hydrogel) as the tested sample groups. All mixtures were oscillated at 25 °C for 3 h. After centrifugation at 12,000 r/min for 5 min, the absorbance of each supernatant was determined at 541 nm with a spectrophotometer (JASCO V-550 UV–Vis, Japan). The percent hemolysis of red blood cells was defined as follows: hemolysis ratio (%) = [(sample absorbance − negative control absorbance)/(positive control absorbance − negative control absorbance)] × 100%. Each experiment was performed in triplicate.

BMP-2 release from the PMMA–hydrogel cement

According to the manufacturer's instructions, the BMP-2 product tube (C012, Novoprotein, Shanghai, China) was centrifuged before opening, and the lyophilized BMP-2 was dissolved in 50 mM acetic acid to prepare a 100 μg/mL BMP-2 solution. Next, PMMA–20% hydrogel hybrid cement with 25 μg/mL BMP-2 was prepared, as described above. This hybrid cement was added to a 1.5 mL microcentrifuge tube with 1 mL PBS at 25 °C and mixed at a speed of 120 r/min. After 12 h and 1, 2, 3, 5, 8, 11, 16, 21, and 26 days, the PBS in the tube was collected and replaced with an equivalent volume of fresh PBS. A BMP-2 ELISA kit (Elabscience, Wuhan, China) was used to measure the concentration of BMP-2 in solution, according to the manufacturer's instructions. The experiments were conducted in triplicate.

Alkaline phosphatase and Alizarin red staining

We measured ALP and Alizarin red staining of BMSCs cultured in extracts of the PMMA–20% hydrogel hybrid cement (BMP-2(-) group) and the PMMA–20% hydrogel hybrid cement with 25 μg/mL BMP-2 (BMP-2(+) group). First, BMSCs were seeded into 24-well plates at a density of 5×10^4 cells per well. The medium was replaced with the experimental extracts after 24 h of culture. After a 5-day incubation, the cells were fixed in 4% paraformaldehyde for 15 min, and ALP staining was performed using an ALP kit (Beyotime), according to the manufacturer's instructions. For Alizarin red staining, cells were incubated with the extracts for 21 days, then fixed in 4% paraformaldehyde for 15 min, and staining performed according to the manufacturer's instructions (Cyagen, Guangzhou, China). Image Pro Plus 6.0 was used to analyze the staining intensity of cells from five different, independent wells.

Assessment of osteogenic marker genes

The expression of BMSC osteogenic marker genes, including *Runx2*, *Col1*, and *OPN*, was assessed using quantitative real-time polymerase chain reaction (qRT-PCR) with a SYBR® Premix Ex TaqTM kit (TaKaRa, Otsu, Japan) and Applied Biosystems 7500 Real-Time PCR System. The following four groups were assessed after incubating BMSCs for 10 days: (1) BMSCs in complete α-MEM medium (control group); (2) complete osteogenic differentiation medium (Cyagen) (P-Control group); (3) extracts of the PMMA–20% hydrogel hybrid cement without BMP-2 (BMP-2(-) group); and (4) extracts of the PMMA–20% hydrogel hybrid cement with 25 μg/mL BMP-2 (BMP-2(+) group). Total RNA was then extracted using a Qiagen RNeasy® Mini kit (Valencia, CA, USA) and subjected to cDNA synthesis. qRT-PCR was performed in triplicate using the following cycling parameters: initial denaturation at 95 °C for 30 s, 40 cycles of denaturation at 95 °C for 5 s, and annealing at 60 °C for 34 s. Glyceraldehyde-3-phosphate dehydrogenase (GAPDH) was used as a quantitative control for the RNA levels. Primer sequences were as follows: *Runx2*, 5′-TCTTCCCAAAGCCAGAGCG-3′ and 5′-TGCCATTCGAGGTGGTCG-3′; *Col1*, 5′-TGACTGGAAGAGCGGAGAGTA-3′ and 5′-GGGGTTTGGGGCTGATGTACC-3′; *OPN*, 5′-GAGGAGAAGGGCGCATTACAG-3′ and 5′-AAACGTCTGCTTGTCTGCTGG-3′; *GAPDH*, 5′-GGCAAGTTCAACGGCACAGT-3′ and 5′- GCCAGTAGACTCCACGACAT-3′.

Osteogenic differentiation assessment

The expression of representative proteins (Runx2 and OPN) of osteogenic differentiation of BMSCs cultured with extract of the BMP-2(-) group or BMP-2(+) group was determined using fluorescence staining [25]. Briefly, BMSCs were seeded into a confocal culture dish at a density of 10^5 cells per dish. The medium was replaced with above extracts after 24 h of culture. After culturing for 12 days, the cells were fixed for 15 min in 4% paraformaldehyde (Biosharp, Hefei, China), followed by treatment with 0.1% Triton-X for 10 min to permeabilize the cells, and then immersed in 1% bovine serum albumin block solution for 1 h. Primary polyclonal IgG rabbit anti-rat Runx2 antibodies (1:500, Abcam, USA) and OPN antibodies (1:200, Abcam) were then added and the preparation was allowed to hybridize overnight at 4 °C. Secondary goat anti-rabbit Alexa Fluor 594 antibody (1:200, Abcam) was then added to the primary antibody for 2 h at 25 °C. The cytoskeleton was stained with Alexa Fluor 488 phalloidin (Thermo Fisher, USA) for 2 h at 25 °C and nuclei were stained with 4′,6-diamidino-2-phenylindole for 5 min at 25 °C. Images were acquired using a fluorescence confocal microscope (Leica, Germany), and Image Pro Plus 6.0 was used to evaluate the fluorescence intensity of Runx2 and OPN of three parallel samples, from five different viewing regions.

In vivo animal study

Previous investigations used New Zealand rabbits to build a femoral condyle bone-defect model for evaluating the biodegradability and osteogenesis capacity of bone cement [26, 27]. Thus, in our study, 20 male New Zealand rabbits (weighing 2.5–3.0 kg) were anesthetized through an intravenous injection of pentobarbital (30 mg/kg). After sterilization, the femoral condyle was exposed using a lateral approach, and a hole (5 mm diameter, 5 mm depth) was made using a hand drill. The rabbits were randomly allocated and treated according to the following four groups ($n = 5$ per group): pure PMMA group; PMMA–15% hydrogel with-

out BMP-2 group; PMMA–20% hydrogel without BMP-2 group; and PMMA–20% hydrogel with BMP-2 group. The incision was closed and antibiotics were used for 3 days after the operation to prevent infection. The rabbits were euthanized 10 weeks post-operation. The femur specimens were excised and the soft tissues were cleared.

All specimens were examined using a microcomputed tomography (micro-CT) scan system (Bruker skyscan1176; Germany) at a spot size of 10 μm, maximum voltage of 40 kV, and a current of 250 μA. The bone volume fraction (bone volume/tissue volume, BV/TV) was calculated using auxiliary software. The excised samples were then fixed in 4% paraformaldehyde, dehydrated in ethanol, and embedded in methyl methacrylate. Hard tissue slicing of the specimens was performed using a microtome (Leica). Finally, sections approximately 40 μm thick were cut, ground, and then subjected to von Kossa (VK) staining using routine methods [28].

Statistics

Statistics were analyzed using statistical product and service solutions (SPSS) version 19.0. Values are shown as the mean ± standard deviation, and were analyzed using one-way analysis of variance and independent *t* tests. Statistical significance was set at $p < 0.05$.

Results

Material characterization of the PMMA–hydrogel hybrid cements

Synthesis of the hybrid cements with PMMA, oxidized hyaluronic acid, and carboxymethyl chitosan hydrogel loaded with BMP-2 is shown in Fig. 1. As the proportion of hydrogel increased, the different hybrid cements became more transparent (Fig. 2a). Similar to pure PMMA cement, all PMMA–hydrogel hybrid cements exhibited an exothermal behavior during setting. All of the PMMA-hydrogel hybrid cements showed a significantly lower maximum setting temperature (T_{max}) than pure PMMA (Fig. 2b). In the present study, the T_{max} of the PMMA–hydrogel cements gradually decreased as the hydrogel content increased; the T_{max} values were 59.10 ± 3.56, 52.73 ± 1.57, 44.07 ± 2.27, 39.57 ± 2.54, and 35.37 ± 1.23 °C for the PMMA–5% hydrogel, PMMA–10% hydrogel, PMMA–15% hydrogel, PMMA–20% hydrogel, and PMMA–25% hydrogel groups, respectively (Fig. 2c). T_{max} is an important precondition that influences the loading of bioactive factors; thus, since the T_{max} of the PMMA–5% hydrogel and PMMA–10% hydrogel groups was more than 50 °C, we excluded these two groups from the subsequent experiments.

The compressive strength of the pure PMMA, PMMA–15% hydrogel, PMMA–20% hydrogel, and PMMA–25% hydrogel groups was approximately 95, 35, 25, and 15 MPa, respectively (Fig. 2d). The compressive strength of the investigated PMMA–hydrogel hybrid cements was lower than that of pure PMMA cement. Since the compressive strength of the PMMA–25% hydrogel group was low, it would be inadequate in providing mechanical support in fractured vertebral bodies; thus, the PMMA–25% hydrogel group was not included in the subsequent experiments. The compression stress–strain curve based on the elastic deformation is shown in Fig. 2d. The Young's modulus of the pure PMMA, PMMA–15% hydrogel, PMMA–20% hydrogel, and PMMA–25% hydrogel groups was 1.59 ± 0.14, 0.41 ± 0.05, 0.28 ± 0.05, and 0.13 ± 0.02 GPa, respectively (Fig. 2e). As the hydrogel content increased, the Young's modulus gradually decreased.

The injectability of the hybrid cement is another important index reflecting its applicability; in this study, it was evaluated by an extrusion test. The injectability of PMMA–hydrogel hybrid cements was lower than that of pure PMMA cement (Fig. 2f). In addition, there were no significant differences between the initial and final setting times of the PMMA–15% hydrogel and PMMA–20% hydrogel groups; both times were shorter than those of the pure PMMA group ($p < 0.05$) (Fig. 2g).

Finally, material degradation was evaluated using an SBF saturation test and examination of bone cements under SEM. After 14 days of soaking of pure PMMA, PMMA–15% hydrogel, and PMMA–20% hydrogel groups, a degraded hole was observed in the PMMA–hydrogel hybrid cements, whereas there were no changes in the micromorphology of the pure PMMA cement (Fig. 3a). At 28 days, the area of the degraded hole in the PMMA–hydrogel hybrid cements obviously increased, and that of the PMMA–20% hydrogel group was greater than that of the PMMA–15% hydrogel group. The calculated degradation rate demonstrated that there was no obvious degradation of pure PMMA, whereas the degradation rate of the PMMA–hydrogel hybrid cements gradually increased with prolonged soaking time (Fig. 3b). In particular, the degradation rate of the PMMA–20% hydrogel group was higher than that of PMMA–15% hydrogel group at the same time point. At 28 days after soaking, the degradation rates of the pure PMMA, PMMA–15% hydrogel, and PMMA–20% hydrogel groups were (0.45 ± 0.09)%, (8.53 ± 0.88)%, and (11.07 ± 1.27)%, respectively.

In vitro cytocompatibility and hemolysis test

The cytocompatibility of pure PMMA, PMMA–15% hydrogel, and PMMA–20% hydrogel groups was monitored for

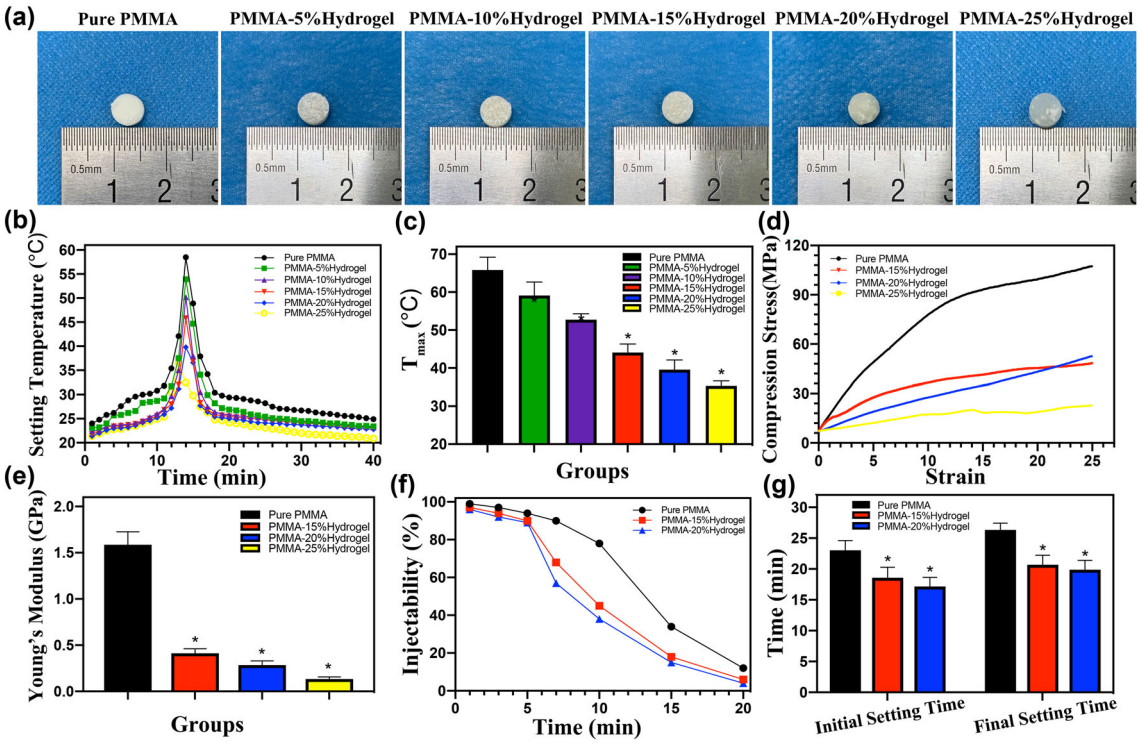

Fig. 2 Characterization of the physical properties of PMMA–hydrogel hybrid cements. **a** Images of the different fabricated cements; **b** curve of setting temperature; **c** maximum setting temperature (T_{max}); **d** compressive strength; **e** Young's modulus; **f** injectability; **g** initial and final setting times ($n = 3$ per group; $^*p < 0.05$ vs. pure PMMA group)

7 days using the CCK-8 test. BMSCs thrived and exhibited excellent proliferation ability when cultured with the extracts of PMMA–hydrogel hybrid cements (Fig. 3c). Further, the proliferation of BMSC proliferation was higher in the PMMA–20% hydrogel group than in the PMMA–15% hydrogel group at different time points. In contrast, when cultured with extract of pure PMMA, BMSCs showed significantly lower proliferation than that of the above two groups ($p < 0.05$). The results of Live-Dead staining showed that more than 90% of the BMSCs were living on day 1 in all groups; in both the PMMA–15% hydrogel and PMMA–20% hydrogel groups, more than 95% were living at days 3, 5, and 7. At above time points, the percentage of live cells days was higher in the PMMA–hydrogel hybrid cements than in the pure PMMA cement ($p < 0.05$), which was consistent with the CCK-8 results (Figs. S1a and S1b in Supplementary Information).

Blood compatibility is a critical index for assessing the biocompatibility of biomaterials, and biocompatibility determines the possible in vivo applications of these bone cements. The supernatants of the pure PMMA cement and PMMA–hydrogel hybrid cements were limpid, and showed no difference compared with that of the negative control group (Fig. 3d), suggesting that the constructed PMMA–hydrogel hybrid cements exhibited good blood compatibility. In addition, the hemolysis rates of both the pure PMMA group and PMMA–hydrogel groups were lower than 4% (Fig. 3e); these rates meet the requirement of ISO/TR7405-1984(E).

BMP-2 release from PMMA–hydrogel hybrid cement

The PMMA–20% hydrogel group exhibited a lower T_{max} than the PMMA–15% hydrogel group; this group also showed good cytocompatibility, which is important for delivering factors and for its use in vivo. Therefore, we used the PMMA–20% hydrogel cement loaded with BMP-2 to evaluate the release of BMP-2 and its osteogenesis ability in vitro and in vivo. BMP-2 was sustainably released over 26 days from the PMMA–20% hydrogel hybrid cement loaded with 25 μg/mL BMP-2 (Fig. 3f).

Evaluation of in vitro osteogenesis ability of PMMA–hydrogel hybrid cements with and without BMP-2

To assess the osteogenesis ability of the PMMA–20% hydrogel hybrid cement with and without BMP-2, BMSCs were cultured with the extracts of these cements. After culturing for 5 days, ALP staining demonstrated significantly higher activity in the BMP-2(+) group than in the BMP-2(-) group

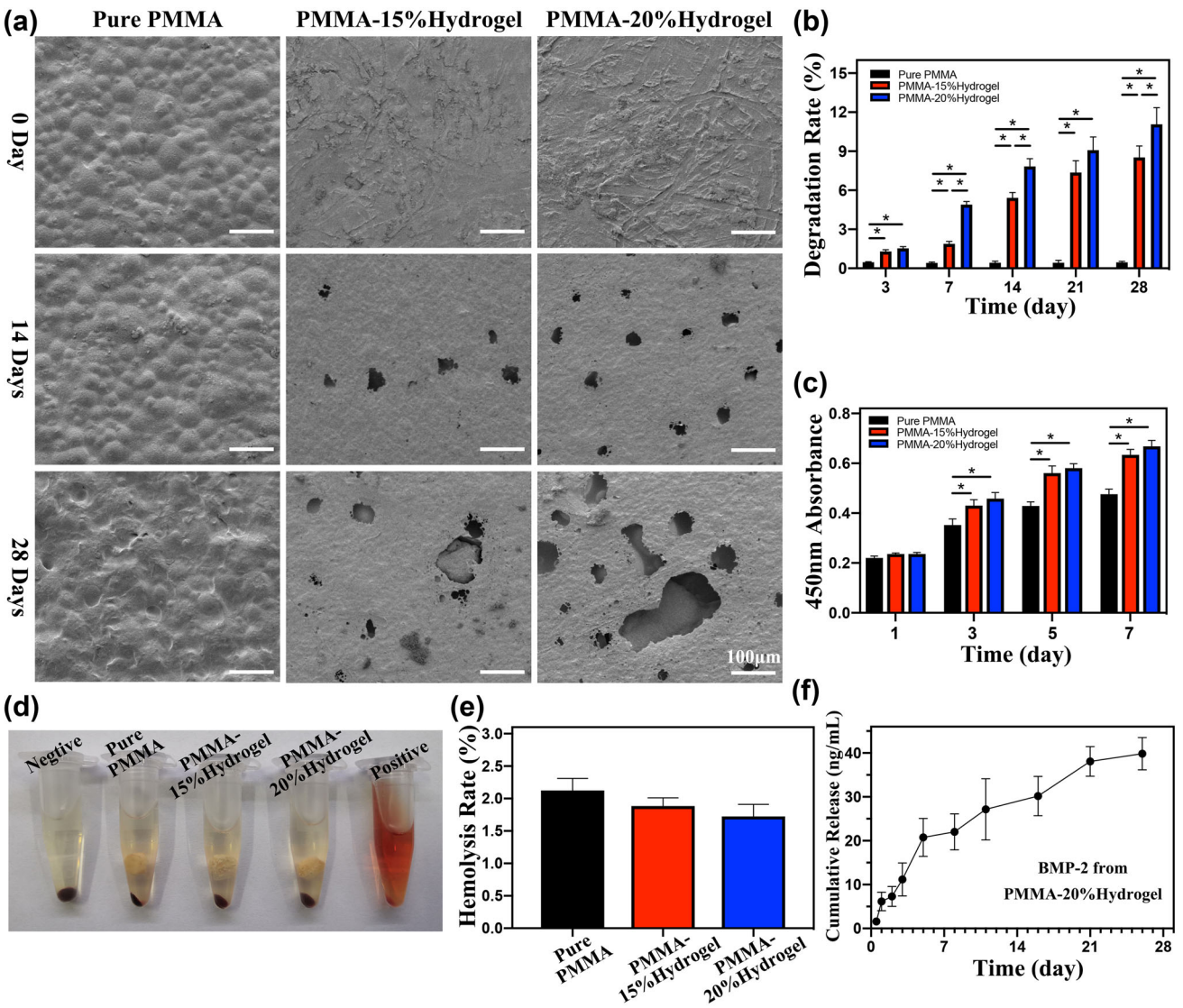

Fig. 3 Biodegradation and biocompatibility of the PMMA–hydrogel hybrid cements and release of loaded BMP-2 from the hybrid cements. **a** SEM images of the surface of the different cements before and after soaking in SBF for 14 and 28 days; **b** degradation ratio (%) of different cements after soaking in SBF for 3, 7, 14, 21, and 28 days; **c** optical density (OD) value of the CCK8 test after cells were cultured in different cement extracts for 1, 3, 5, and 7 days; **d** photographs of direct observations of the hemolysis test results; **e** hemolysis rate; **f** cumulative release of BMP-2 from the PMMA–20% hydrogel hybrid cement at different times ($n = 3$ per group; $^*p < 0.05$)

(Figs. 4a and 4b; $p < 0.05$). qRT-PCR showed that expressions of the osteogenic genes *Runx2*, *Col1*, and *OPN* were relatively similar in the control and BMP-2(-) groups. However, compared with expression in the BMP-2(-) group, the expression of these genes was significantly higher in the BMP-2(+) group (Figs. 4d–4f; $p < 0.05$). After culturing for 12 days, immunofluorescence staining revealed higher expression of the Runx2 and OPN proteins in the BMP-2(+) group than the BMP-2(-) group (Figs. 5a–5d; $p < 0.05$). Furthermore, to evaluate the mineralization level of BMSCs, Alizarin red staining was conducted at 21 days; more red calcified nodules were observed in the BMP-2(+) group than in the BMP-2(-) group (Figs. 4a and 4c; $p < 0.05$).

Evaluation of in vivo osteogenesis ability of PMMA–hydrogel hybrid cements with and without BMP-2 by micro-CT analysis

At 10 weeks post-surgery, the pure PMMA cement showed bulky distribution patterns that did not cause changes in the morphology, whereas the PMMA–hydrogel hybrid cements exhibited obvious degradation with the formation of sev-

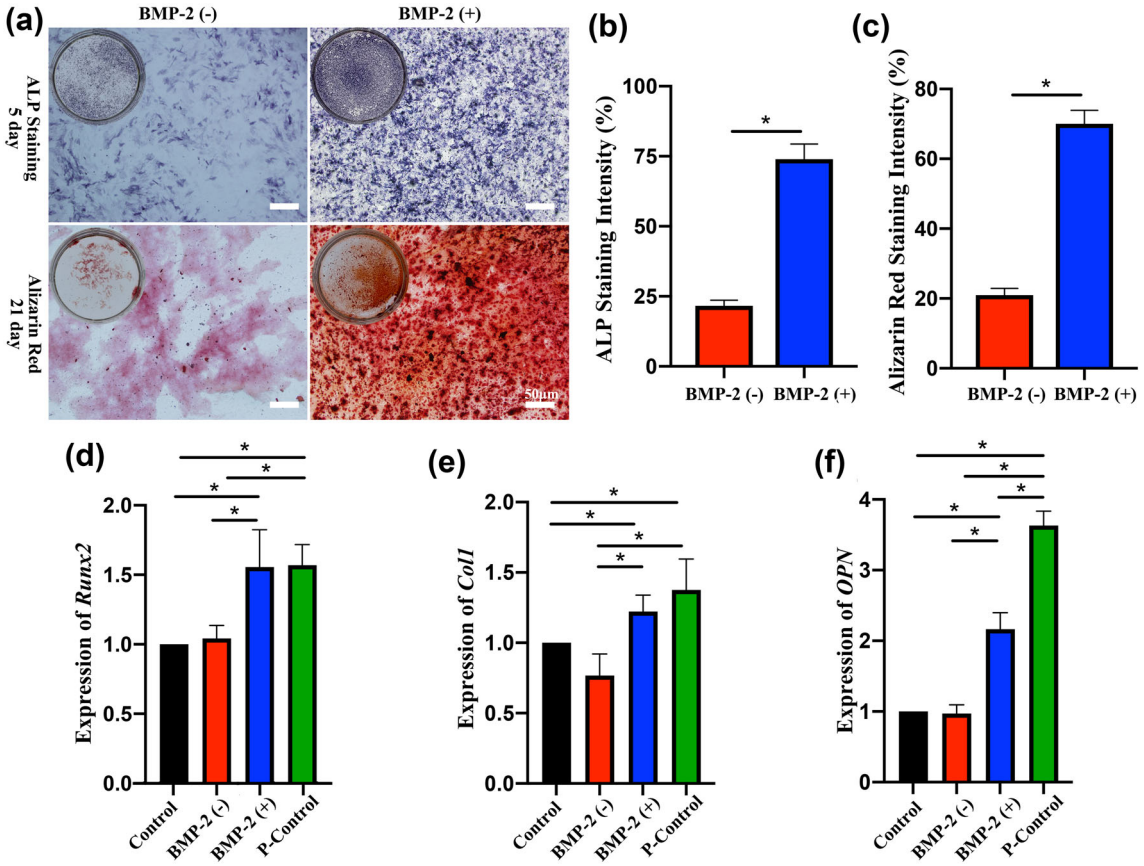

Fig. 4 Evaluation of in vitro osteogenesis ability of PMMA–hydrogel hybrid cements with or without added BMP-2. **a** Images of ALP and Alizarin red staining; **b, c** quantitative analysis of ALP and Alizarin red staining; **d-f** qRT-PCR analysis of *Runx2*, *Col1*, and *OPN* gene expression. BMP-2(-) group and BMP-2(+) group refer to PMMA–20% hydrogel hybrid cement without and with BMP-2, respectively. Control indicates BMSCs cultured in α-MEM medium; P-Control indicates BMSCs cultured in osteogenic medium (*$p < 0.05$)

eral micropores (Fig. 6a). In addition, newly formed bone was observed in the interior of the injected bone cement, with a CT value similar to that of the surrounding bone. These results can be observed in the micro-CT images (new bone marked with the green arrows in Fig. 6). We calculated the BV/TV to further quantify the repair of the femoral condyle defects in rabbits injected with pure PMMA cement or PMMA–hydrogel hybrid cement with or without BMP-2. The BV/TV value of PMMA–20% hydrogel with BMP-2 group was significantly higher than that in the pure PMMA group, PMMA–15% hydrogel without BMP-2 group, and PMMA–20% hydrogel without BMP-2 group (Fig. 6b; $p < 0.05$).

Histological staining analysis

To assess effects of treatments on bone repair, we carried out VK staining on femoral condyle sections. At 10 weeks post-surgery, higher rates of new bone formation were observed in rabbits injected with the PMMA–hydrogel hybrid cements than those injected with pure PMMA cement (new bone is marked with green arrows in Fig. 7). In addition, there was more new bone tissue in the PMMA–20% hydrogel with BMP-2 group than that in the PMMA–20% hydrogel without BMP-2 group. In summary, micro-CT and histological staining results demonstrate the excellent osteogenesis capacity of the PMMA–20% hydrogel with BMP-2 group.

Discussion

Currently, PMMA cement is widely used in PVP and PKP [1–3]. However, bioinert PMMA cement does not facilitate bone tissue regeneration [6, 8]. In this regard, we constructed novel PMMA–hydrogel hybrid cements loaded with BMP-2 to promote osteogenesis. Analysis of our fabricated PMMA–hydrogel hybrid cements with BMP-2 showed that they exhibit promising potential for clinical applications.

In clinical practice, restoration of the stability of fractured vertebral bodies is one of the most important goals

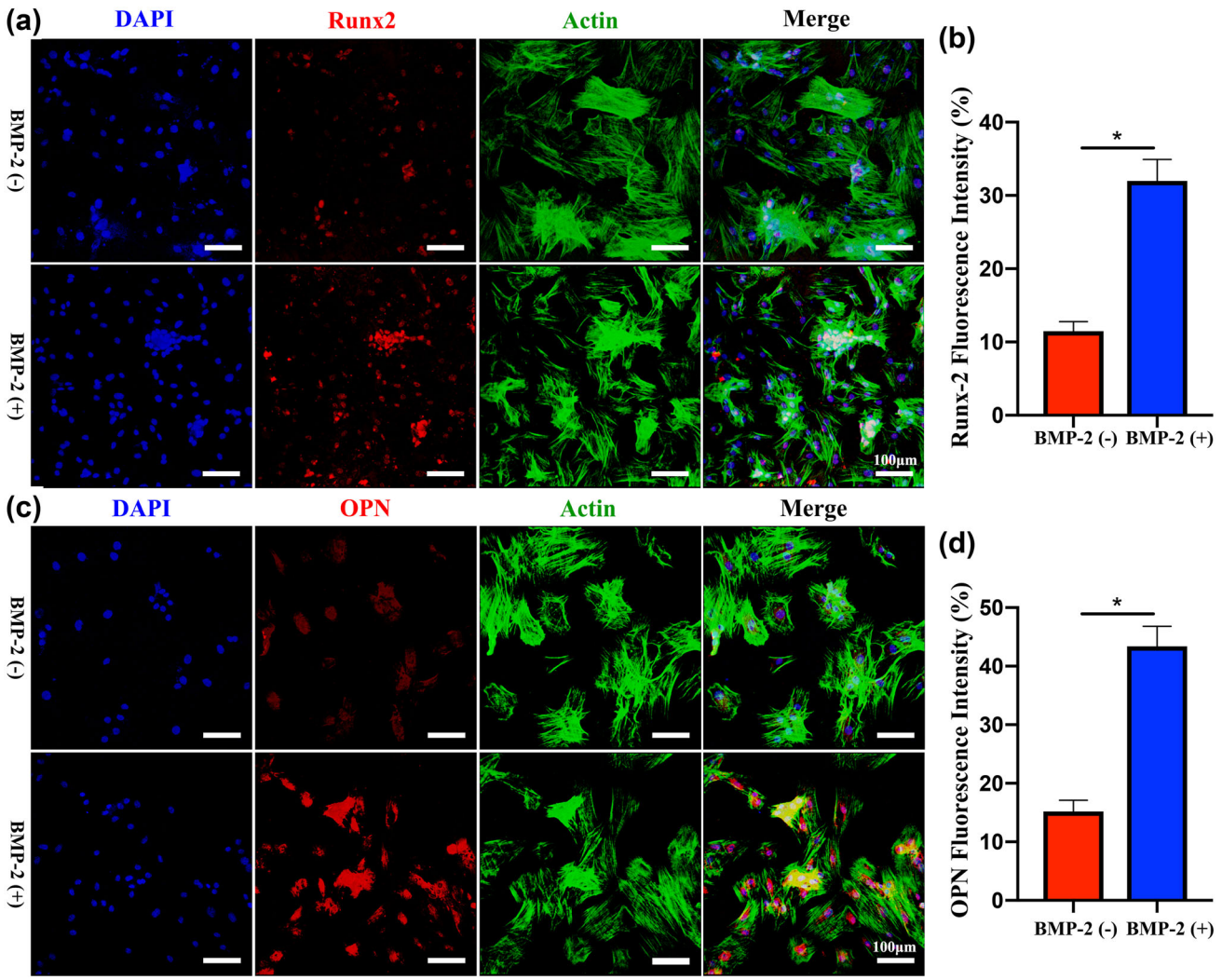

Fig. 5 Immunofluorescence staining and quantitative analysis of Runx2 and OPN protein expression in BMSCs. **a, b** Images and quantitative analysis of Runx-2; **c, d** images and quantitative analysis of OPN. BMP-2(-) group and BMP-2(+) group refer to PMMA–20% hydrogel hybrid cement without and with BMP-2, respectively (*$p < 0.05$)

of PVP or PKP in the treatment of OVCFs, which can also help maintain vertebral height over the long term. Although PMMA can effectively stabilize fractured vertebral bodies, it shows extremely high stiffness (1700–3700 MPa), which is significantly higher than that of natural vertebral bodies (10–900 MPa) [6, 29–31]. Thus, PMMA cement increases the risk of side effects after PVP or PKP, such as intervertebral disk degeneration and new fractures in adjacent vertebrae [32–35]. In our study, the addition of oxidized hyaluronic acid and carboxymethyl chitosan hydrogel to the PMMA matrix successfully moderated the Young's modulus of the hybrid cements by decreasing the PMMA content. In addition, owing to the degradative nature of hydrogel, PMMA–hydrogel hybrid cements showed good biodegradability as evaluated by SEM and in vitro degradation tests. Specifically, SEM revealed obvious hole formation on the surface of PMMA–hydrogel hybrid cements at 14 and 28 days of soaking. In particular, the degradation rate of the PMMA–20% hydrogel group after soaking for 28 days was $(11.07 \pm 1.27)\%$. With the partial degradation of the hydrogel, there was space for new bone formation. Furthermore, when cultured with the extract of the PMMA–hydrogel hybrid cements, BMSCs showed greater growth and proliferation viability than when cultured with textracts of pure PMMA cement, as confirmed using the CCK-8 test and Live-Dead staining. These results indicate that PMMA–hydrogel hybrid cements have better biocompatibility than pure PMMA cement. The hemolysis test results revealed hemolysis rates of all groups to be less than 4%, which met the ISO/TR7405-1984(E) standard.

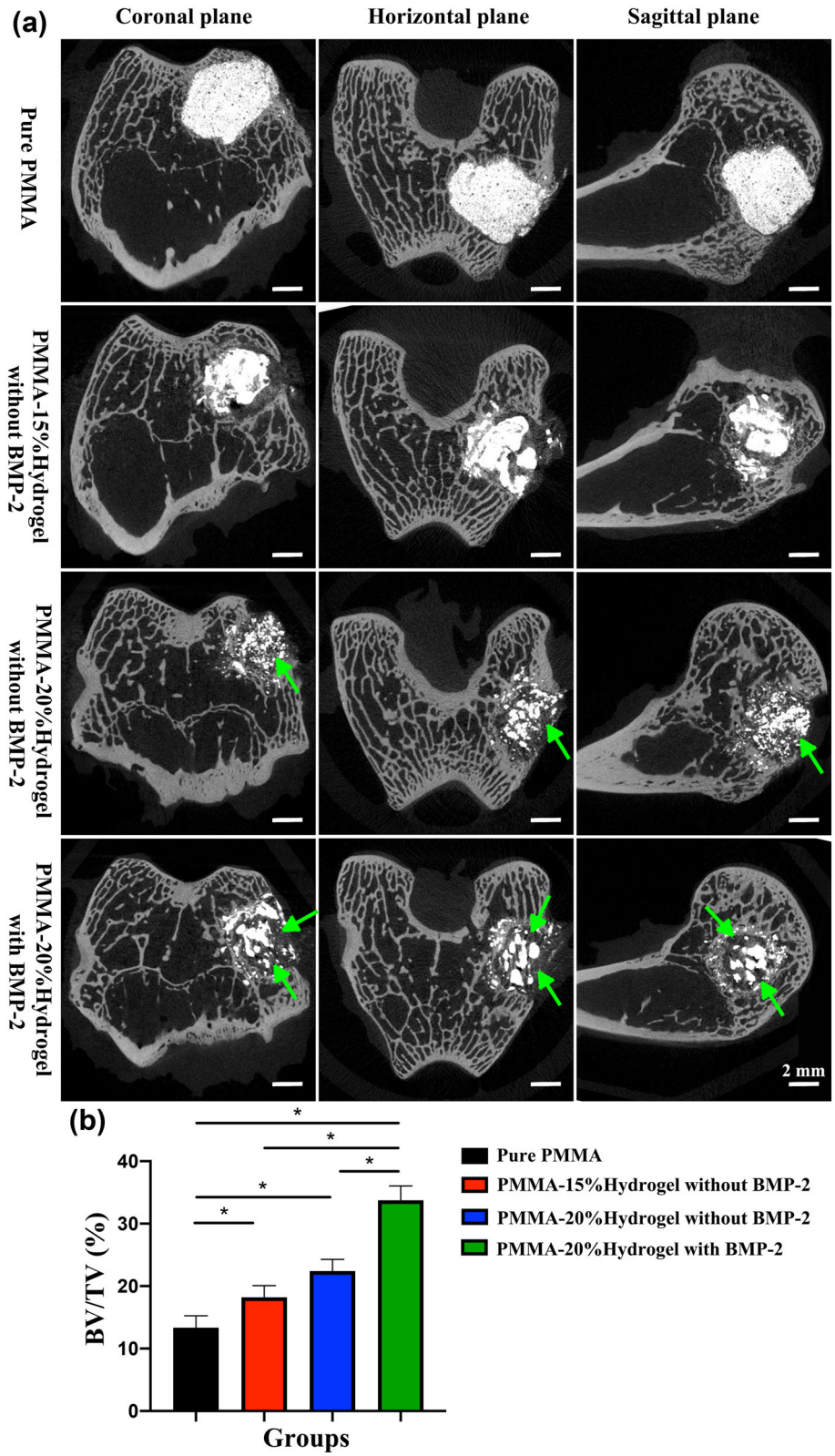

Fig. 6 Micro-CT examination of different groups in vivo. **a** Micro-CT images (the green arrow indicates the new bone in bone cement); **b** calculated bone volume/tissue volume (BV/TV) ($n = 5$ per group; $^*p < 0.05$)

Sufficient mechanical strength of bone cements is important in preventing vertebral height loss, further reducing the risk of kyphosis after surgery [3, 36]. In our study, the compression strength of the PMMA–20% Hydrogel group was approximately 25 MPa, which is higher than that of normal cortical bone and cancel-

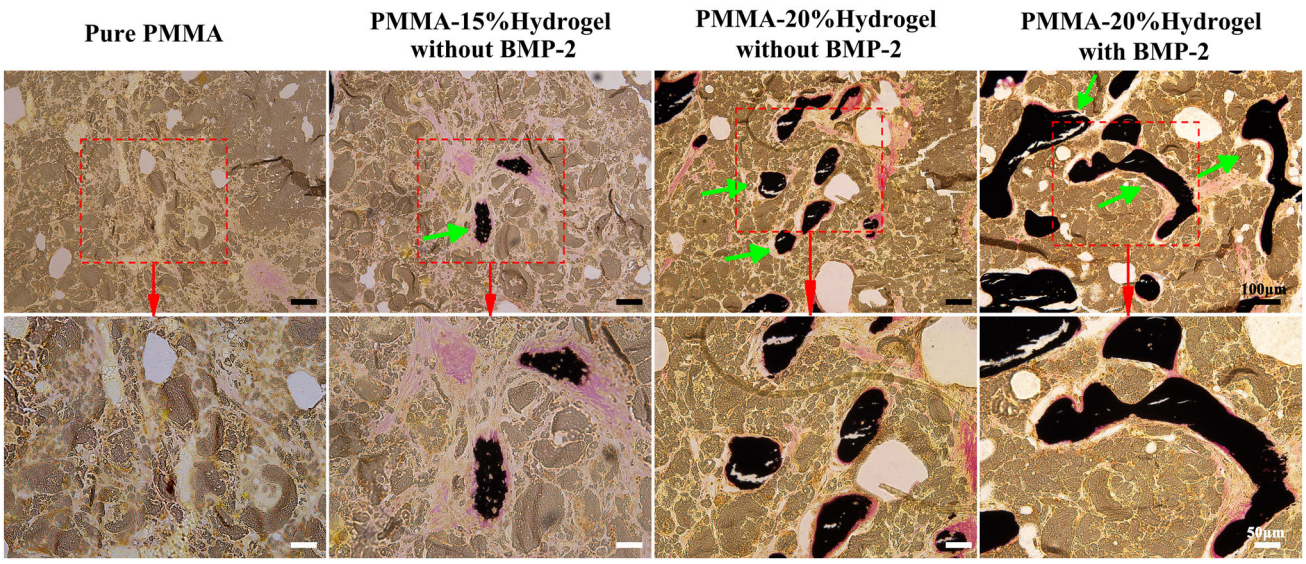

Fig. 7 von Kossa staining of different groups in vivo. The green arrow indicates the new bone in the bone cement. The background is bone cement in bone defects

lous bone (approximately 0.1–15 MPa) [30, 37]. The synthesized PMMA–hydrogel hybrid cements in our study exhibited better compression strength than that of PMMA/chitosan–glycerophosphate/nanosized hydroxyapatite hydrogel hybrid cements (approximately 5 MPa) and that of PMMA/hydroxyapatite/carboxymethylcellulose hydrogel hybrid cements (approximately 10 MPa) [15, 17]. Therefore, the composite PMMA–hydrogel hybrid cements in the present study might meet the clinical requirements for mechanical strength for treatment of OVCFs with PVP and PKP.

PMMA is a biologically inert material that provides mechanical support for fractured vertebral bodies but cannot accelerate osteogenesis or fracture union. Chiu et al. reported that PMMA cement also suppresses the expression of transcription factors that accelerate osteoprogenitor differentiation and inhibit osteoprogenitor viability [38, 39]. As a result, fracture non-union may lead to persistent back pain, Kummell's disease, and loose bone cement, which may cause protrusion of the bone cement into the spinal canal after a second trauma [3]. Previous studies reported that the addition of HA, silicate bioceramic, and bioactive glass to PMMA cement could promote osteogenesis [6, 11, 12]. For example, HA can improve the generation of extracellular matrixes, growth factors, and serum proteins, and facilitate the adherence of the osteogenic cells [11, 40]. Moreover, HA and silicon iron enhance mesenchymal stem cell proliferation and osteogenic differentiation, osteoblast activity, and mineralization of intercellular substances [6, 11, 12]. However, the osteogenesis ability of the above materials is significantly lower than that of bioactive factors, such as BMPs.

There have no previous studies on the effects of addition of bioactive factors to PMMA cement; in particular, setting temperatures that are higher than 60 °C could result in bone tissue necrosis and inactivate bioactive factors [14]. In addition, PMMA cement does not provide a suitable liquid environment for loading bioactive factors; after setting the bone cement, its non-degradable nature restricts the release of bioactive factors. Sa et al. and Wang et al. reported that PMMA–hydrogel hybrid cements with different ratios have lower setting temperatures, typically less than 40 °C [15, 17]. In our study, the setting temperature of the PMMA–hydrogel hybrid cements was lower than that of pure PMMA cement ($p < 0.05$); specifically, the mixture setting temperature of the PMMA–20% hydrogel group was 39.57 ± 2.54 °C, which is low enough to retain bioactivity of osteogenic factors. The lower setting temperature of the synthesized hybrid cement can be attributed to the reduced amount of PMMA cement and decalescence of the hydrogel.

BMP-2, a member of the superfamily of transforming growth factor beta, is a well-known osteogenic factor that can promote osteogenic differentiation of osteoblasts and BMSCs by activating the BMP/Smad1/5/8 signaling pathway by up-regulating the expression of ALP, Runx2, and OPN [21, 22]. Numerous studies have reported that hydrogels can load and release BMP-2 [41–43]. In this study, we added BMP-2 to oxidized hyaluronic acid and carboxymethyl chitosan hydrogel, and then added the mixture to the PMMA cement, thereby obtaining novel PMMA–hydrogel hybrid cements loaded with BMP-2. In addition to the lower setting temperature of the PMMA–hydrogel hybrid cements, and the suitable and biodegrable hydrogel, BMP-2 could be

released from the hybrid cements in our study, further promoting osteogenesis.

In our in vitro study, PMMA–20% hydrogel hybrid cement with BMP-2 promoted the expression of osteogenesis-related marker genes or factors, as confirmed by ALP staining, immunofluorescence staining, Alizarin red staining, and qRT-PCR. The results revealed that release of BMP-2 by the PMMA–hydrogel hybrid cements can stimulate BMSC osteogenesis [21, 22]. In our in vivo experiments, micro-CT and histological staining were used to observe biodegradation and new bone formation. Ten weeks after implantation into the femoral condyle of rabbits, these observations revealed not only that the PMMA–hydrogel hybrid cements are biodegradable, but also that with the addition of BMP-2 to the PMMA–hydrogel hybrid cements, there was obvious new bone formation in the interior of the injected bone cement in bone defects. Therefore, we suggest that the bioactive BMP-2 released from our novel PMMA–hydrogel hybrid cements with BMP-2 can promote BMSC osteogenesis differentiation and accelerate fracture union.

Conclusions

In summary, we constructed novel PMMA-oxidized hyaluronic acid and carboxymethyl chitosan hydrogel hybrid cements loaded with BMP-2. The synthesized PMMA–hydrogel hybrid cements exhibited a low setting temperature and Young's modulus; acceptable mechanical strength, injectability, and setting time; and excellent biodegradability and biocompatibility. Importantly, BMP-2 was sustainably released from the PMMA–hydrogel hybrid cements, demonstrating their good bioactivity in enhancing BMSCs osteogenesis and accelerating new bone formation in the implant area. Therefore, the constructed PMMA–hydrogel hybrid cements loaded with BMP-2 show promising potential for use in PVP and PKP for the treatment of OVCFs in clinical practice.

Supplementary Information The online version contains supplementary material available at https://doi.org/10.1007/s42242-021-00172-1.

Acknowledgements This work was supported by the National Key R&D Program of China (No. 2018YFA0703000), the National Natural Science Foundation of China (Nos. 82071564, 82072412, and 81772326), the Fundamental Research Program Funding of Ninth People's Hospital Affiliated to Shanghai Jiao Tong University School of Medicine (No. JYZZ070), and Project of Shanghai Science and Technology Commission (No. 19XD1434200/18431903700).

Author contributions JWW, HYL, WJJ, KPS, and YKG were involved in conceptualization; XS, XZ, and WJJ helped in data curation; XS, XZ, and XJ contributed to formal analysis; JWW, WJJ, and XS were involved in funding acquisition; JWW, HYL, and WJJ helped in investigation; XS, XZ, XJ, JM, XZL, and HY contributed to methodology; JWW, HYL, and WJJ were involved in project administration; JWW, HYL, and WJJ helped in supervision; JWW, HYL, and WJJ contributed to validation; XS, XZ, XJ, JM, XZL, and HY were involved in writing—original draft; JWW, HYL, WJJ, KPS, YKG, XS, XZ, and XJ helped in writing—review & editing.

Declarations

Conflict of interest The authors declare that there is no conflict of interest.

Ethical approval All animal procedures and the use of animals in our study were approved by Shanghai Ninth People's Hospital, Shanghai Jiao Tong University School of Medicine Animal Care and Use Committee and complied with the guidelines of the National Institutes of Health Guide for Care and Use of Laboratory Animals (GB14925-2010).

Availability of data and material The datasets used or analyzed during the current study are available from the corresponding authors on reasonable request.

References

1. Lou S, Shi X, Zhang X et al (2019) Percutaneous vertebroplasty versus non-operative treatment for osteoporotic vertebral compression fractures: a meta-analysis of randomized controlled trials. Osteoporos Int 30(12):2369–2380. https://doi.org/10.1007/s00198-019-05101-8
2. Chang X, Lv YF, Chen B et al (2015) Vertebroplasty versus kyphoplasty in osteoporotic vertebral compression fracture: a meta-analysis of prospective comparative studies. Int Orthop 39(3):491–500. https://doi.org/10.1007/s00264-014-2525-5
3. Sun X, Liu X, Wang J et al (2020) The effect of early limited activity after bipedicular percutaneous vertebroplasty to treat acute painful osteoporotic vertebral compression fractures. Pain Phys 23(1):E31-E40
4. Melton LJ (1997) Epidemiology of spinal osteoporosis. Spine 22(24 Suppl):2s–11s. https://doi.org/10.1097/00007632-199712151-00002
5. Felsenberg D, Silman AJ, Lunt M et al (2002) Incidence of vertebral fracture in europe: results from the European Prospective Osteoporosis Study (EPOS). J Bone Miner Res 17(4):716–724. https://doi.org/10.1359/jbmr.2002.17.4.716
6. Sun X, Wu Z, He D et al (2019) Bioactive injectable polymethylmethacrylate/silicate bioceramic hybrid cements for percutaneous vertebroplasty and kyphoplasty. J Mech Behav Biomed Mater 96:125–135. https://doi.org/10.1016/j.jmbbm.2019.04.044
7. Lu Q, Liu C, Wang D et al (2019) Biomechanical evaluation of calcium phosphate-based nanocomposite versus polymethylmethacrylate cement for percutaneous kyphoplasty. Spine J 19(11):1871–1884. https://doi.org/10.1016/j.spinee.2019.06.007
8. Cui X, Huang C, Zhang M, et al. (2017) Enhanced osteointegration of poly(methylmethacrylate) bone cements by incorporating strontium-containing borate bioactive glass. J R Soc Interf 14(131):20161057. https://doi.org/10.1098/rsif.2016.1057
9. Khandaker M, Vaughan MB, Morris TL et al (2014) Effect of additive particles on mechanical, thermal, and cell functioning properties of poly(methyl methacrylate) cement. Int J Nanomed 9:2699–2712. https://doi.org/10.2147/ijn.S61964
10. Zhang CL, Shen GQ, Zhu KP et al (2016) Biomechanical effects of morphological variations of the cortical wall at the bone-cement interface. J Orthop Surg Res 11(1):72. https://doi.org/10.1186/s13018-016-0405-y

11. Aghyarian S, Rodriguez LC, Chari J et al (2014) Characterization of a new composite PMMA-HA/Brushite bone cement for spinal augmentation. J Biomater Appl 29(5):688–698. https://doi.org/10.1177/0885328214544770
12. Goñi I, Rodríguez R, García-Arnáez I et al (2018) Preparation and characterization of injectable PMMA-strontium-substituted bioactive glass bone cement composites. J Biomed Mater Res B Appl Biomater 106(3):1245–1257. https://doi.org/10.1002/jbm.b.33935
13. Zhang J, Zhou H, Yang K et al (2013) RhBMP-2-loaded calcium silicate/calcium phosphate cement scaffold with hierarchically porous structure for enhanced bone tissue regeneration. Biomaterials 34(37):9381–9392. https://doi.org/10.1016/j.biomaterials.2013.08.059
14. Li S, Chien S, Brånemark PI (1999) Heat shock-induced necrosis and apoptosis in osteoblasts. J Orthop Res 17(6):891–899. https://doi.org/10.1002/jor.1100170614
15. Sa Y, Yang F, de Wijn JR et al (2016) Physicochemical properties and mineralization assessment of porous polymethylmethacrylate cement loaded with hydroxyapatite in simulated body fluid. Mater Sci Eng C Mater Biol Appl 61:190–198. https://doi.org/10.1016/j.msec.2015.12.040
16. Meng B, Qian M, Xia SX et al (2013) Biomechanical characteristics of cement/gelatin mixture for prevention of cement leakage in vertebral augmentation. Eur Spine J 22(10):2249–2255. https://doi.org/10.1007/s00586-013-2886-2
17. Lin HH, Chang MC, Wang ST et al (2018) The fates of pedicle screws and functional outcomes in a geriatric population following polymethylmethacrylate augmentation fixation for the osteoporotic thoracolumbar and lumbar burst fractures with mean ninety five month follow-up. Int Orthop 42(6):1313–1320. https://doi.org/10.1007/s00264-018-3812-3
18. Thambi T, Li Y, Lee DS (2017) Injectable hydrogels for sustained release of therapeutic agents. J Contr Release 267:57–66. https://doi.org/10.1016/j.jconrel.2017.08.006
19. Gorantla S, Waghule T, Rapalli VK et al (2019) Advanced hydrogels based drug delivery systems for ophthalmic delivery. Recent Pat Drug Deliv Formul 13(4):291–300. https://doi.org/10.2174/1872211314666200108094851
20. Li L, Wang N, Jin X et al (2014) Biodegradable and injectable in situ cross-linking chitosan-hyaluronic acid based hydrogels for postoperative adhesion prevention. Biomaterials 35(12):3903–3917. https://doi.org/10.1016/j.biomaterials.2014.01.050
21. Chen Z, Zhang Z, Ma X et al (2019) Newly designed human-like collagen to maximize sensitive release of BMP-2 for remarkable repairing of bone defects. Biomolecules 9(9):450. https://doi.org/10.3390/biom9090450
22. Ryoo HM, Lee MH, Kim YJ (2006) Critical molecular switches involved in BMP-2-induced osteogenic differentiation of mesenchymal cells. Gene 366(1):51–57. https://doi.org/10.1016/j.gene.2005.10.011
23. Yang J, Zhang K, Zhang S, et al (2015) Preparation of calcium phosphate cement and polymethyl methacrylate for biological composite bone cements. Med Sci Monit 21:1162–1172. https://doi.org/10.12659/msm.893845
24. Liu Z, Pu F, Huang S et al (2013) Long-circulating Gd_2O_3:Yb^{3+}, Er^{3+} up-conversion nanoprobes as high-performance contrast agents for multi-modality imaging. Biomaterials 34(6):1712–1721. https://doi.org/10.1016/j.biomaterials.2012.11.009
25. Sun X, Ma Z, Zhao X et al (2021) Three-dimensional bioprinting of multicell-laden scaffolds containing bone morphogenic protein-4 for promoting M2 macrophage polarization and accelerating bone defect repair in diabetes mellitus. Bioact Mater 6(3):757–769. https://doi.org/10.1016/j.bioactmat.2020.08.030
26. Zhang X, Kang T, Liang P et al (2018) Biological activity of an injectable biphasic calcium phosphate/pmma bone cement for induced osteogensis in rabbit model. Macromol Biosci 18(3):1700331. https://doi.org/10.1002/mabi.201700331
27. Zhu T, Ren H, Li A et al (2017) Novel bioactive glass based injectable bone cement with improved osteoinductivity and its in vivo evaluation. Sci Rep 7(1):3622. https://doi.org/10.1038/s41598-017-03207-9
28. Galovich LA, Perez-Higueras A, Altonaga JR et al (2011) Biomechanical, histological and histomorphometric analyses of calcium phosphate cement compared to PMMA for vertebral augmentation in a validated animal model. Eur Spine J 20 (Suppl 3):376–382. https://doi.org/10.1007/s00586-011-1905-4
29. Boger A, Bohner M, Heini P et al (2008) Properties of an injectable low modulus PMMA bone cement for osteoporotic bone. J Biomed Mater Res B Appl Biomater 86(2):474–482. https://doi.org/10.1002/jbm.b.31044
30. Helgason B, Perilli E, Schileo E et al (2008) Mathematical relationships between bone density and mechanical properties: a literature review. Clin Biomech 23(2):135–146. https://doi.org/10.1016/j.clinbiomech.2007.08.024
31. Chen L, Tang Y, Zhao K et al (2019) Fabrication of the antibiotic-releasing gelatin/PMMA bone cement. Colloids Surf B Biointerf 183:110448. https://doi.org/10.1016/j.colsurfb.2019.110448
32. Zhao H, Ni CF, Huang J et al (2014) Effects of bone cement on intervertebral disc degeneration. Exp Ther Med 7(4):963–969. https://doi.org/10.3892/etm.2014.1531
33. Kim SH, Kang HS, Choi JA et al (2004) Risk factors of new compression fractures in adjacent vertebrae after percutaneous vertebroplasty. Acta Radiol 45(4):440–445. https://doi.org/10.1080/02841850410005615
34. Feng Z, Chen L, Hu X et al (2018) Vertebral augmentation can induce early signs of degeneration in the adjacent intervertebral disc: evidence from a rabbit model. Spine 43(20):E1195–E1203. https://doi.org/10.1097/brs.0000000000002666
35. Lee WS, Sung KH, Jeong HT et al (2006) Risk factors of developing new symptomatic vertebral compression fractures after percutaneous vertebroplasty in osteoporotic patients. Eur Spine J 15(12):1777–1783. https://doi.org/10.1007/s00586-006-0151-7
36. Wang C, Zhang X, Liu J et al (2019) Percutaneous kyphoplasty: risk factors for recollapse of cemented vertebrae. World Neurosurg 130:e307–e315. https://doi.org/10.1016/j.wneu.2019.06.071
37. Nazarian A, von Stechow D, Zurakowski D et al (2008) Bone volume fraction explains the variation in strength and stiffness of cancellous bone affected by metastatic cancer and osteoporosis. Calcif Tissue Int 83(6):368–379. https://doi.org/10.1007/s00223-008-9174-x
38. Chiu R, Smith KE, Ma GK et al (2010) Polymethylmethacrylate particles impair osteoprogenitor viability and expression of osteogenic transcription factors Runx2, osterix, and Dlx5. J Orthop Res 28(5):571–577. https://doi.org/10.1002/jor.21035
39. Zhu J, Yang S, Cai K et al (2020) Bioactive poly (methyl methacrylate) bone cement for the treatment of osteoporotic vertebral compression fractures. Theranostics 10(14):6544–6560. https://doi.org/10.7150/thno.44428
40. Dutta SR, Passi D, Singh P et al (2015) Ceramic and non-ceramic hydroxyapatite as a bone graft material: a brief review. Ir J Med Sci 184(1):101–106. https://doi.org/10.1007/s11845-014-1199-8
41. Wang B, Guo Y, Chen X et al (2018) Nanoparticle-modified chitosan-agarose-gelatin scaffold for sustained release of SDF-1 and BMP-2. Int J Nanomed 13:7395–7408. https://doi.org/10.2147/ijn.S180859

42. Chen D, Zhao M, Mundy GR (2004) Bone morphogenetic proteins. Growth Factors 22(4):233–241. https://doi.org/10.1080/08977190412331279890

43. Jung T, Lee JH, Park S et al (2017) Effect of BMP-2 delivery mode on osteogenic differentiation of stem cells. Stem Cells Int 2017:7859184. https://doi.org/10.1155/2017/7859184